ELSEVIER

Journal of Alloys and Compounds 408–412 (2006) 1429–1433

Journal of ALLOYS AND COMPOUNDS

www.elsevier.com/locate/jallcom

Electromagnetic wave absorption properties of iron/rare earth oxide composites dispersed by amorphous carbon powder

DeShan Li, Takashi Horikawa, JiuRong Liu, Masahiro Itoh, Ken-ichi Machida *

Center for Advanced Science and Innovation, Osaka University, 2-1 Yamadaoka, Suita, Osaka 565-0871, Japan

Available online 31 May 2005

Abstract

The sludge powders of Nd–Fe–B sintered magnets were oxidized at 250–325 °C for 2 h and then the α-Fe/Fe_2B/Nd_2O_3/amorphous carbon (a-C) nanocomposite powders were prepared by ball-milling the sludge with the a-C powder for 12–40 h. The resin composites of 75 mass% of these nanocomposite powders showed excellent electromagnetic wave absorption properties in GHz range. The effective absorption of RL <−20 dB were observed in a range of 7.6–18.0 GHz and the minimum absorption peaks around −58.5 dB appeared at 12.0 GHz with matching thickness of 1.9 mm for the samples heated at 300 °C for 2 h and then ball-milled with 4.8 mass% a-C for 30 h.

Keywords: Nd–Fe–B sintered magnets; Amorphous carbon; Nanocomposites; Ball-milling; Electromagnetic wave absorption

1. Introduction

Recently, the electromagnetic wave (EM) absorbing materials have been attracting much attention because the electromagnetic interference problems become more common along with the rapid development and spread of electronic devices using the electromagnetic wave in GHz range. An establishment of the electromagnetic compatibility (EMC), improvements in noise resistance and suppressions of radiation of useless noises, in or between those devices are an urgent and serious problems. For these EMC problems, various kinds of ferrite materials with spinel-type crystal structure were mainly used as impedance elements or EM absorbing materials. In high frequency range, however, large permeability values can hardly be expected for these spinel-type ferrites because of the Snoek's limit [1]. Therefore, it is possible to produce the materials with excellent EM absorbing properties by using metal magnetic materials with large saturation magnetization than such ferrites, and by suppressing the generation of reflux magnetic domains or eddy current through down-sizing them to the finer particles.

Sugimoto et al. [2,3] have reported the α-Fe/SmO composite powders which possess good microwave absorption properties (RL <−20 dB) in 0.73–1.30 GHz range, and good microwave absorption properties of the α-Fe/Y_2O_3 nanocomposite at 2.0–3.5 GHz were demonstrated by our previous study [4]. In these works, both nanocomposite materials were prepared by the hydrogen disproportionation process for rare-earth intermetallic compounds, Sm_2Fe_{17} and Y_2Fe_{17}, followed by the oxidation for forming the rare-earth oxides as insulators, SmO or Y_2O_3, which increase the electrical resistivity owing to their effective isolation for α-Fe particles. Present authors have also developed an efficient recovery procedure for the sludge powders of Nd–Fe–B sintered magnets to nanocomposite powders of α-Fe/Fe_2B/Nd_2O_3 as EM absorbing materials in the GHz range by similar disproportionation processes [5].

The loss of the high-frequency permeability (W) for magnetic materials by the eddy current is expressed as follows:

$$W = \frac{\pi^2 I^2 d^2 f^2}{6\rho} \quad (1)$$

where I is the magnetization, d the thickness of the material, f the frequency and ρ is the electrical resistivity. Through the improvement of electrical resistivity, the present authors have recently discovered that the amorphous carbon (a-C) with low

* Corresponding author. Tel.: +81 6 6879 4209; fax: +81 6 6879 4209.
E-mail address: machida@casi.osaka-u.ac.jp (K.-i. Machida).

0925-8388/$ – see front matter © 2005 Published by Elsevier B.V.
doi:10.1016/j.jallcom.2005.04.109

electrical conductivity in α-Fe/a-C or Fe_2B/a-C nanocomposites plays a role as an insulating barrier to enhance the electrical resistivity [6,7]. In addition, Rochman et al. have reported the decrease in crystallite size of Fe mechanically alloyed with fine graphite powders [8]. A smaller crystallite size will also help to suppress the eddy current induced in Fe fine particles. The purpose of this study is to prepare the α-Fe/Fe_2B/Nd_2O_3/a-C nanocomposite powders by dispersing the disproportionated sludge powders of Nd–Fe–B sintered magnets into a-C powders with a ball-milling, and to investigate the relationships between resulting electromagnetic wave absorbing properties and the characteristics of nanocomposite materials such as microstructures, compositions as well as preparation conditions.

2. Experimental

For raw materials, the sludge powder (particle size = 1–4 μm) produced from Nd–Fe–B sintered magnets and a-C (particle size = 1–4 μm) were used. Firstly, 10 g of sludge powders were heated at 250–325 °C for 2 h with ball-milling type electric furnace in air. Resultant powders and 4.8 mass% of a-C were then put into a container for the ball-milling together with a surfactant (Aerosol OT), 10 steel balls (Ø 9.5 mm) and 10 ml of *n*-hexane. After a ball-milling at 200 rpm for 12–40 h, powders obtained were washed by *n*-hexane several times, and then dried in vacuo at room temperature.

The crystal structures of powders were characterized by X-ray diffraction (XRD, RIGAKU, RINT2200), the microstructures were analyzed using a scanning electron microscope (SEM, HITACHI, S-3000HXS), and the oxygen content was measured on an oxygen/nitrogen analyzer (HORIBA, EMGA-550). The epoxy resin composites of 75 mass% of powders were pressed into disc-shaped compacts of 2.0 ± 0.5 mm thickness. These compacts were heated at 170 °C for 30 min in air and then were cut into toroidal shaped samples (Ø out = 7.00 and Ø in = 3.04 mm) using an ultrasonic cutter (CHO-ONPA KOUGYOU). The *S* parameters for these resin composites were measured by the coaxial method using a vector network analyzer (Agilent Technologies 8720ES) at 0.05–18.0 GHz range. The relative complex permeability ($\mu_r = \mu'_r - j\mu''_r$) and permittivity ($\varepsilon_r = \varepsilon'_r - j\varepsilon''_r$) were evaluated by these parameters, and the electromagnetic wave absorption properties were calculated as a frequency dependence of reflection loss (RL) at a thickness by using μ_r and ε_r according to the following equations:

$$Z_{in} = Z_0 \left(\frac{\mu_r}{\varepsilon_r}\right)^{\frac{1}{2}} \tanh\left\{ j\left(\frac{2\pi f d}{c}\right)(\mu_r \varepsilon_r)^{\frac{1}{2}} \right\} \quad (2)$$

$$RL = 20 \log\left|\frac{Z_{in} - Z_0}{Z_{in} + Z_0}\right| \quad (3)$$

where *f* is the frequency of the microwave, *d* the thickness of an absorber, Z_0 the impedance of air and *c* is the velocity of the light.

3. Results and discussion

Fig. 1 shows the XRD patterns for (a) raw sludge powders, (b) as-oxidized at 300 °C for 2 h, (c and d) as-milled powders for 20 and 30 h, respectively. The XRD pattern for raw sludge powders was assigned to $Nd_2Fe_{14}B$ (tetragonal), and after oxidation at 300 °C for 2 h, a broad peak around $2\theta = 44°$ and weak peaks at $2\theta = 63°$ and 81° were indexed as (1 1 0), (2 0 0) and (2 1 1) reflections of α-Fe, respectively. Weak peaks around $2\theta = 30°$ were assigned to Nd_2O_3, indicating that the α-Fe/Fe_2B/Nd_2O_3 nanocomposite powders were formed according to the following reaction equation:

$$Nd_2Fe_{14}B + \tfrac{3}{2}O_2 \rightarrow Nd_2O_3 + 12Fe + Fe_2B$$

The peaks from Fe_2B were not detected in the XRD pattern so that the crystallinity was poor or the formation amount was small. For the heating temperature at 250 °C, the oxidation was insufficient and the peaks of Nd_2Fe_4B still remained in the XRD pattern. On the other hand, the oxidation completely finished at 325 °C and excess oxygen content values were detected for the resultant powders (7.29 wt.%), suggesting that the Fe component became oxidized. The oxygen content of powders treated at 300 °C (4.95 wt.%) was close to that calculated as all Nd components were oxidized (4.25 wt.%). From these results, the composite powders oxidized at 300 °C were used for further investigations.

The α-Fe/Fe_2B/Nd_2O_3/a-C nanocomposite powders were obtained after ball-milling with a-C as reported elsewhere [6]. For these nanocomposite powders, the XRD patterns were al-

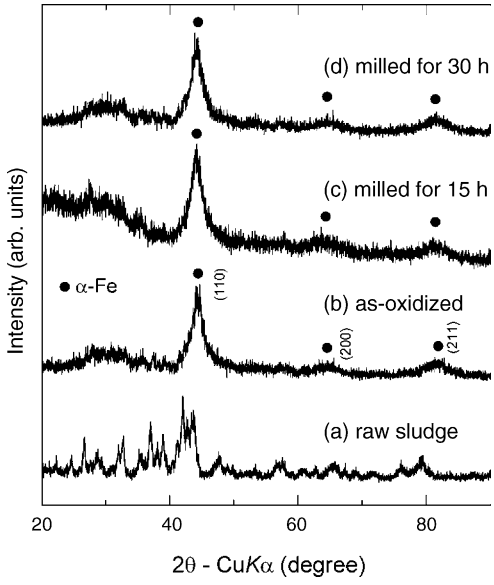

Fig. 1. XRD patterns for sample powders: (a) raw sludge, (b) as-oxidized at 300 °C for 2 h and (c and d) ball-milled with 4.8 mass% of a-C for 15 and 30 h, respectively.

most similar to those of the samples ball-milled up to 25 h and the typical pattern is shown in Fig. 1(c). A broad peak of a-C, weak peaks of Nd_2O_3 and three peaks of α-Fe were observed at the 2θ angles around 28°, 30°, 44°, 63° and 81°, respectively. Meanwhile, the XRD pattern was changed by extending the ball-milling time for 30 h, as shown in Fig. 1(d). The decrease in the relative peak intensity of a-C to α-Fe (see Fig. 1(d)) presumably suggests some improvements in the uniformity of α-Fe/Fe_2B/Nd_2O_3/a-C nanocomposite powders, and the diffusion of carbon from the a-C particles to the grain boundaries of α-Fe/Fe_2B/Nd_2O_3 nanocomposite particles was performed by further extending the ball-milling time similar to the cases of α-Fe/a-C or Fe_2B/a-C nanocomposite particles [6]. A similar tendency was also observed on the SEM images shown in Fig. 2. For the as-oxidized sludge powder (Fig. 2(a)), the particle size distribution of the α-Fe/Fe_2B/Nd_2O_3 nanocomposite powders (3–10 μm) was decreased to about 2–5 μm with increasing the ball-milling time to 20 h and finally average particle size of about 1 μm was attained after 30 h (see Fig. 2(b and c)). In addition, Fig. 2(c) showed us after that the nanocomposite powder particles are uniformly dispersed together with the a-C powders after 30 h of ball-milling. For more detail discussions, transmission electron microscope (TEM) observations for these nanocomposite powders are in progress.

The EM absorbing properties for resin composites of 75 mass% of nanocomposite powders studied are summarized in Table 1. The frequency dependences of imaginary part (μ_r'') of relative permeability for the resin composites of nanocomposite powders of α-Fe/Fe_2B/Nd_2O_3 and ball-milled α-Fe/Fe_2B/Nd_2O_3/a-C for 15, 20, 30 and 40 h were plotted in Fig. 3. While the μ_r'' value for α-Fe/Fe_2B/Nd_2O_3 nanocomposite powders gave a maximum peak of 0.8 around 6 GHz, broad peaks with maximum values at different frequencies between 6–11 GHz were observed for ball-milled α-Fe/Fe_2B/Nd_2O_3/a-C nanocomposite powders. Additionally, the μ_r'' value of these latter composites was increased with the ball-milling time up to 30 h and then decreased after 40 h.

Fig. 4 shows the frequency dependence of resulting RL values for the resin composites of α-Fe/Fe_2B/Nd_2O_3 powders. Efficient EM absorbing properties (RL <−20 dB) were observed at 4.5–8.3 GHz range, and the minimum peak of −46.7 dB appeared at a matching frequency (f_m) and thickness (d_m) of 6.4 GHz and 2.0 mm, respectively. For the resin

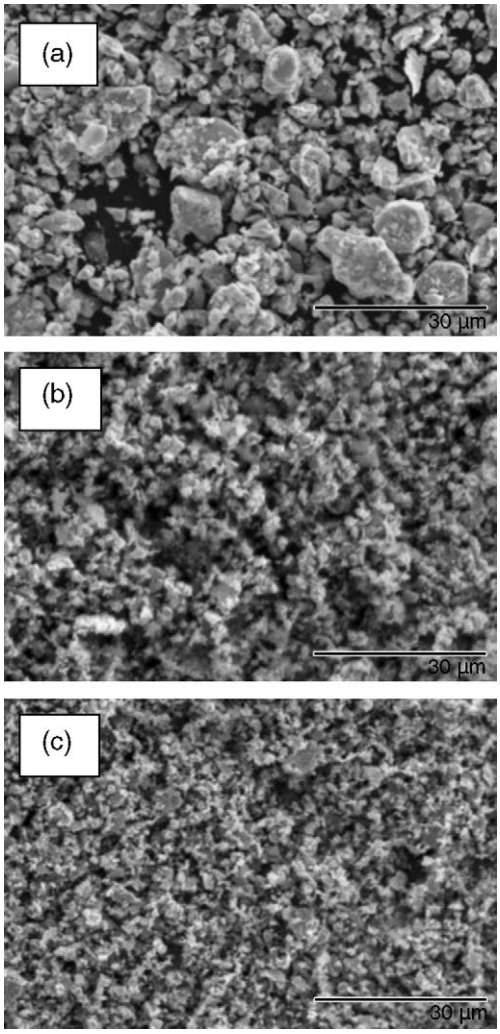

Fig. 2. SEM images for sample powders: (a) α-Fe/Fe_2B/Nd_2O_3/a-C nanocomposite and (b and c) α-Fe/Fe_2B/Nd_2O_3/a-C nanocomposite ball-milled with 4.8 mass% of a-C for 20 and 30 h, respectively.

composites of α-Fe/Fe_2B/Nd_2O_3/a-C nanocomposite powders studied here, since the deviation in their RL values mainly depended on the variation of the μ_r'' values, the highest μ_r'' value, which was obtained after the ball-milling for 30 h, resulted in the most excellent EM absorbing properties as listed in Table 1 and Fig. 5. Compared to the α-Fe/Fe_2B/Nd_2O_3 resin composite in Fig. 4, the frequency re-

Table 1
Types of nanocomposites, milling time and the electromagnetic wave absorption properties for resin composites with 75 mass% of sample powders

Type of nanocomposite	Milling time (h)	Electromagnetic wave absorption properties for resin composites			
		Minimum RL (dB)	f_m (GHz) (minimum RL)	d_m (mm) (RL <−20 dB)	Frequency range (GHz) (RL <−20 dB)
α-Fe/Fe_2B/Nd_2O_3	0 (as-oxidized)	−46.7	6.4	2.1–3.6	3.6–7.0
α-Fe/Fe_2B/Nd_2O_3/a-C	15	−23.8	13.6	1.6–2.3	11.0–17.2
	20	−29.9	14.4	1.5–2.5	8.4–18.0
	30	−58.5	12.0	1.5–2.8	7.6–18.0
	40	−45.2	9.9	1.4–3.0	6.5–18.0

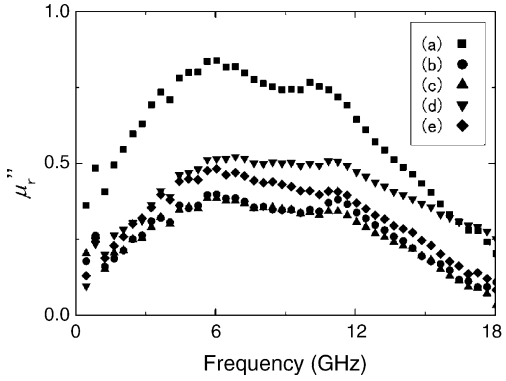

Fig. 3. Frequency dependence of imaginary part of the relative permittivity for the resin composites with 75 mass% of sample powders: (a) as-oxidized at 300 °C for 2 h and (b–e) α-Fe/Fe_2B/Nd_2O_3/a-C nanocomposite powders ball-milled for 15, 20, 30 and 40 h, respectively.

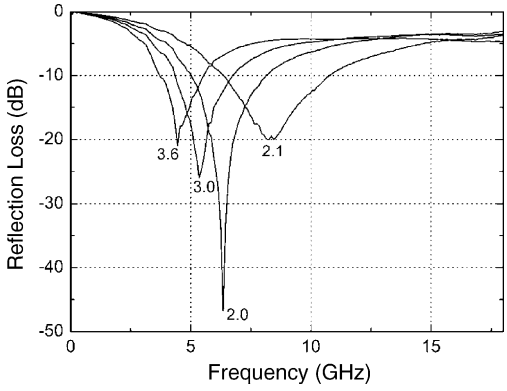

Fig. 4. Frequency dependence of the RL values for the resin composites with 75 mass% of α-Fe/Fe_2B/Nd_2O_3 nanocomposite powders. Numbers represent the thickness of EM absorbing materials.

gion of RL <−20 dB was greatly extended from 4.5–8.3 GHz to 7.6–18.0 GHz, and the minimum RL value of −58.5 dB was obtained at f_m = 12.0 GHz and d_m = 1.9 mm.

The excellent EM absorbing properties are responsible for the following improvements: during a milling time up to 30 h, α-Fe/Fe_2B/Nd_2O_3 nanocomposite and a-C powders are effectively down-sized as well as the nanocomposite powders are dispersed and isolated by the a-C fine particles, and finally the carbon of a-C diffuses through the grain boundaries of α-Fe/Fe_2B/Nd_2O_3 nanocomposite particles as shown in Figs. 1(d) and 2(c). Although the μ_r'' value is decreased due to the dilution effect induced by the addition of a-C as shown in Fig. 3, the electrical resistivity is enhanced, because the a-C powder plays a role as the insulator. As a result, the μ_r'' value improves along with the milling time up to 30 h due to the effective suppression of the eddy current in Fe fine particles. Moreover, the peak shifts to the higher frequency in the μ_r'' and RL curves are supposedly ascribable to the large H_A value of Fe_3C, as suggested by Zhang and Yu [9], formed at these ball-milling processes [8,10]. However, the ball-milling time is prolonged to 40 h, the Fe_3C are formed excessively and the μ_r'' value comes to decrease due to the much smaller saturation magnetization of Fe_3C, 8.2 emu/g [11], than that of α-Fe (215 emu/g). From the high μ_r'' value at 18 GHz and the tendency of RL curves in Fig. 5, efficient EM absorbing properties (RL <−20 dB) are expected at the frequency range above 18 GHz for the resin composite of α-Fe/Fe_2B/Nd_2O_3/a-C nanocomposite powders.

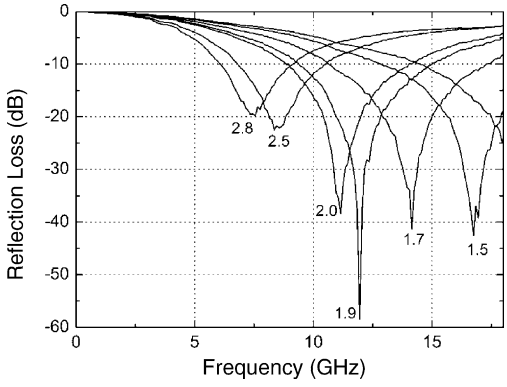

Fig. 5. Frequency dependence of the RL values for the resin composites with 75 mass% of α-Fe/Fe_2B/Nd_2O_3/a-C nanocomposite powders ball-milled for 30 h. Numbers represent the thickness of EM absorbing materials.

4. Conclusions

The conclusions obtained in this study are as follows:

1. The α-Fe/Fe_2B/Nd_2O_3 nanocomposite powders derived from the sludge powders of Nd–Fe–B sintered magnets by the oxidation at 300 °C for 2 h are promising as EM absorbing material, which shows good absorbing properties in the 4.5–8.5 GHz range
2. The resin composites of α-Fe/Fe_2B/Nd_2O_3/a-C nanocomposite powders prepared by ball-milling with 4.8 mass% of a-C show the better EM absorbing properties than α-Fe/Fe_2B/Nd_2O_3 nanocomposite powders at 6.5–18.0 GHz, and the further excellent absorption also is expected in the range above 18 GHz.
3. By optimizing the ball-milling time (30 h), the high EM absorbing properties are obtained due to the electrical resistivity of α-Fe/Fe_2B/Nd_2O_3/a-C nanocomposite powders increased by the uniform dispersion of α-Fe and Fe_2B metallic particles for the nanocomposite powders by a-C.
4. The amorphous carbon (a-C) with low electrical conductivity plays an important a role as the insulating separator to the decrease in permeability caused by the eddy current induced in Fe fine particles.

References

[1] J.L. Snoek, Physica 14 (1948) 207.
[2] T. Maeda, S. Sugimoto, T. Kagotani, D. Book, M. Homma, H. Ota, Y. Houjou, Mater. Trans. 41 (2000) 1172.
[3] S. Sugimoto, T. Maeda, D. Book, T. Kagotani, K. Inomata, M. Homma, H. Ota, Y. Houjou, R. Sato, J. Alloys Compd. 330 (2002) 301.

[4] J.R. Liu, M. Itoh, K. Machida, Chem. Lett. 32 (No. 4) (2003) 394.
[5] K. Machida, M. Masuda, M. Itoh, T. Horikawa, Chem. Lett. 32 (No. 7) (2003) 658.
[6] J.R. Liu, M. Itoh, T. Horikawa, K. Machida, J. Phys. D Appl. Phys. 37 (2004) 2737.
[7] J.R. Liu, M. Itoh, T. Horikawa, H. Mori, K. Machida, Appl. Phys. A, submitted for publication.
[8] N.T. Rochman, K. Kawamoto, H. Sueyoshi, Y. Nakamura, T. Nishida, J. Mater. Proc. Tech. 89–90 (1999) 367.
[9] G.L. Zhang, S. Yu, Phys. Lett. A 222 (1996) 203.
[10] S.J. Campbell, G.M. Wang, A. Calka, W.A. Kaczmarek, Mater. Sci. Eng. A226–228 (1997) 75.
[11] S.I. Nikitenko, Y. Koltypin, I. Felner, I. Yeshurun, A.I. Shames, J.Z. Jiang, V. Markovich, G. Gorodetsky, A. Gedanken, J. Phys. Chem. B 108 (2004) 7620.